



LAWRENCE
LIVERMORE
NATIONAL
LABORATORY

Oxidation/Reduction Reactions at the Metal Contact-TiBr Interface: An X-ray Photoelectron Spectroscopy Study

A. J. Nelson, E. L. Swanberg, L. F. Voss, R. T. Graff, A.
M. Conway, R. J. Nikolic, S. A. Payne, H. Kim, L.
Cirignano, K. Shah

August 1, 2014

SPIE Optics & Photonics
San Diego, CA, United States
August 17, 2014 through August 21, 2014

Disclaimer

This document was prepared as an account of work sponsored by an agency of the United States government. Neither the United States government nor Lawrence Livermore National Security, LLC, nor any of their employees makes any warranty, expressed or implied, or assumes any legal liability or responsibility for the accuracy, completeness, or usefulness of any information, apparatus, product, or process disclosed, or represents that its use would not infringe privately owned rights. Reference herein to any specific commercial product, process, or service by trade name, trademark, manufacturer, or otherwise does not necessarily constitute or imply its endorsement, recommendation, or favoring by the United States government or Lawrence Livermore National Security, LLC. The views and opinions of authors expressed herein do not necessarily state or reflect those of the United States government or Lawrence Livermore National Security, LLC, and shall not be used for advertising or product endorsement purposes.

Oxidation/Reduction Reactions at the Metal Contact-TlBr Interface: An X-ray Photoelectron Spectroscopy Study

A.J. Nelson^{*a}, E.L. Swanberg^a, L.F. Voss^a, R.T. Graff^a, A.M. Conway^a, R.J. Nikolic^a, S.A. Payne^a, H. Kim^b, L. Cirignano^b, and K. Shah^b

^aLawrence Livermore National Laboratory, Livermore, CA, USA

^bRadiation Monitoring Devices, Watertown, MA, USA

ABSTRACT

TlBr radiation detector operation degrades with time at room temperature and is thought to be due to electromigration of Tl and Br vacancies within the crystal as well as the metal contacts migrating into the TlBr crystal itself due to electrochemical reactions at the metal/TlBr interface. X-ray photoemission spectroscopy (XPS) was used to investigate the metal contact surface/interfacial structure on TlBr devices. Device-grade TlBr was polished and subjected to a 32% HCl etch to remove surface damage prior to Mo or Pt contact deposition. High-resolution photoemission measurements on the Tl 4f, Br 3d, Cl 2p, Mo 3d and Pt 4f core lines were used to evaluate surface chemistry and non-equilibrium interfacial diffusion. Results indicate that anion substitution at the TlBr surface due to the HCl etch forms $\text{TlBr}_{1-x}\text{Cl}_x$ with consequent formation of a shallow heterojunction. In addition, a reduction of Tl^{1+} to Tl^0 is observed at the metal contacts after device operation in both air and N_2 at ambient temperature. Understanding contact/device degradation versus operating environment is useful for improving radiation detector performance.

Keywords: Thallium bromide, photoelectron spectroscopy, radiation detection

1. INTRODUCTION

The development of room temperature radiation detectors requires new materials with large band gaps and high atomic number species. Thallium bromide (TlBr) meets these requirements having a wide band gap (2.68 eV), high Z (^{81}Tl) along with high resistivity ($>10^{10} \Omega\text{-cm}$). In addition, TlBr has long carrier lifetimes ($>10\mu\text{s}$, $\mu\tau_e > 5 \times 10^{-3} \text{ cm}^2/\text{V}$) and a demonstrated energy resolution of 1.2% at 662 keV.¹⁻⁴ However, TlBr detectors are susceptible to polarization phenomena that limit long term performance.⁵ It has also been observed that device operation results in the formation of a dark halo around the cathode contact.

Methods to control this polarization must address vacancy migration, surface chemistry and interfacial reactions at the contacts. Native oxides, surface stoichiometry and surface defects due to polishing all affect device performance.⁶ The long-term room temperature stability of TlBr gamma detectors has been improved using surface chemical modification^{7,8} but the operational environment must also be addressed.

This paper assesses and discusses oxidation/reduction reactions and lateral surface compositional variations at and near the metal contacts on HCl treated TlBr operated in air and dry N_2 . The surface chemistry and speciation at the Mo and Pt contacts and across the surface between contacts was examined using X-ray photoelectron spectroscopy (XPS). The operational stability as a function of processing and environment and using these to control the interfacial ionic conductivity has been elucidated with this experimental study.

2. EXPERIMENTAL

Device-grade TlBr samples were polished and immersed in 32% HCl followed by a methanol rinse in air to remove surface damage prior to Mo and Pt contact deposition. Electron beam physical vapor deposition (EBPVD) was used to deposit the metal contacts in a vacuum chamber with a base pressure of 8×10^{-7} torr. Depositions were performed at ambient temperature and at a rate of 0.1 nm/sec for a final contact thickness of 200 nm.

Quantitative compositional analysis of the surface chemistry at the contacts and across the surface between contacts was performed with XPS using a monochromatic Al $K\alpha$ source (1486.7 eV). The 200 μm X-ray beam was incident normal to the sample and the detector is 45° from normal. Core-level spectra were collected with pass energy of 23.5 eV, giving an energy resolution of 0.3 eV that when combined with the 0.85 eV full width half maximum (FWHM) Al $K\alpha$ line width gives a resolvable XPS peak width of 1.2 eV. Deconvolution of non-resolved peaks was accomplished using Multipak 9.2 (PHI) curve fitting routines with Gaussian-Lorentzian line-shapes and a Shirley background. The collected data were referenced to an energy scale with binding energies for Cu $2p_{3/2}$ at 932.72 \pm 0.05 eV and Au $4f_{7/2}$ at 84.01 \pm 0.05 eV. Binding energies were also referenced to the C 1s photoelectron line arising from adventitious carbon at 284.6 eV.⁹

3. RESULTS AND DISCUSSION

Optical photomicrographs of the Pt anodes on TlBr devices operated in air and in N_2 at 200V for 7 days (voltage applied between the two pictured contacts) are presented in Figure 1. The numbered regions of interest (ROI) between the contacts are shown on the photomicrographs. Note that the spot size is 200 μm and the distance between electrodes is 3 mm.

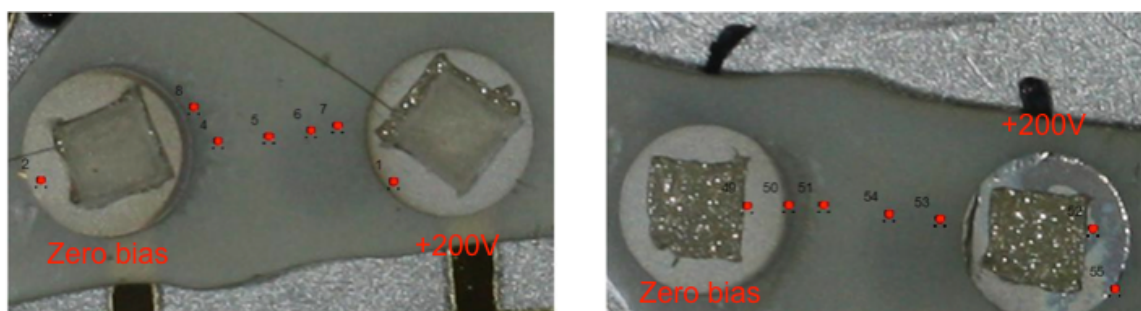


Figure 1. Photomicrographs of Pt/TlBr devices operated (a) in air and (b) in N_2 .

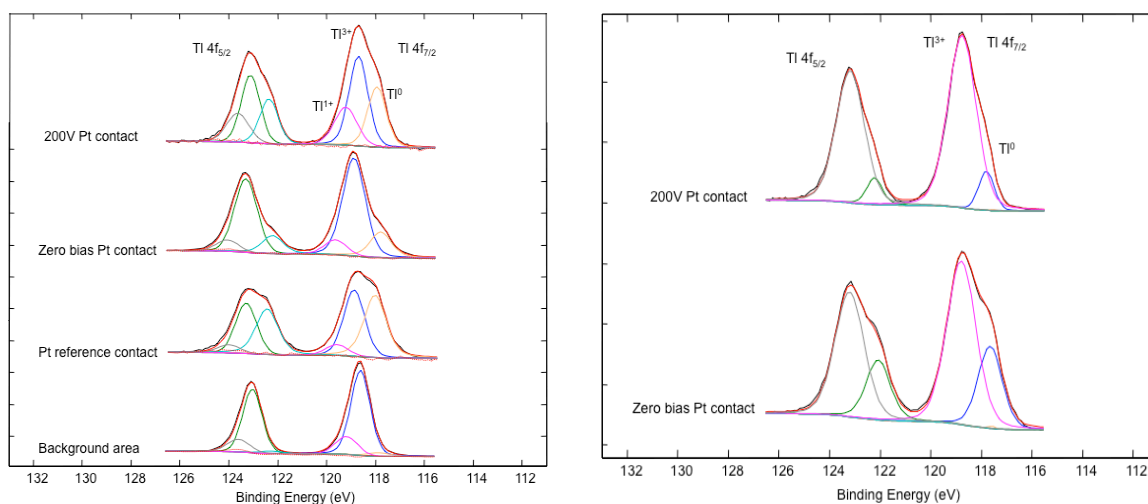


Figure 2. Tl $4f_{7/2,5/2}$ core-level spectra of select sites on TlBr with Pt anodes operated in (a) air and in (b) N_2 at 200V, ambient temperature.

The Tl 4f core-level spectra for Pt anodes operated in air and in N_2 are presented in Figure 2. Curve fitting of the Tl $4f_{7/2,5/2}$ spin-orbit pair shows three peaks indicative of Tl^0 , Tl^{3+} as Tl_2O_3 and Tl^{1+} in TlBr. [10] The Tl 4f spectrum for the background shows an oxidized TlBr surface. Note that Tl is detected on the surface of all the Pt contacts and that the Pt reference contact has a significant Tl^0 component. These spectra represent

an observation of electrocatalytic oxidation/reduction reactions at the Pt/TIBr interface during prolonged device operation. No oxidation/reduction reactions were evident in the Pt 4f spectra and thus are not present here.

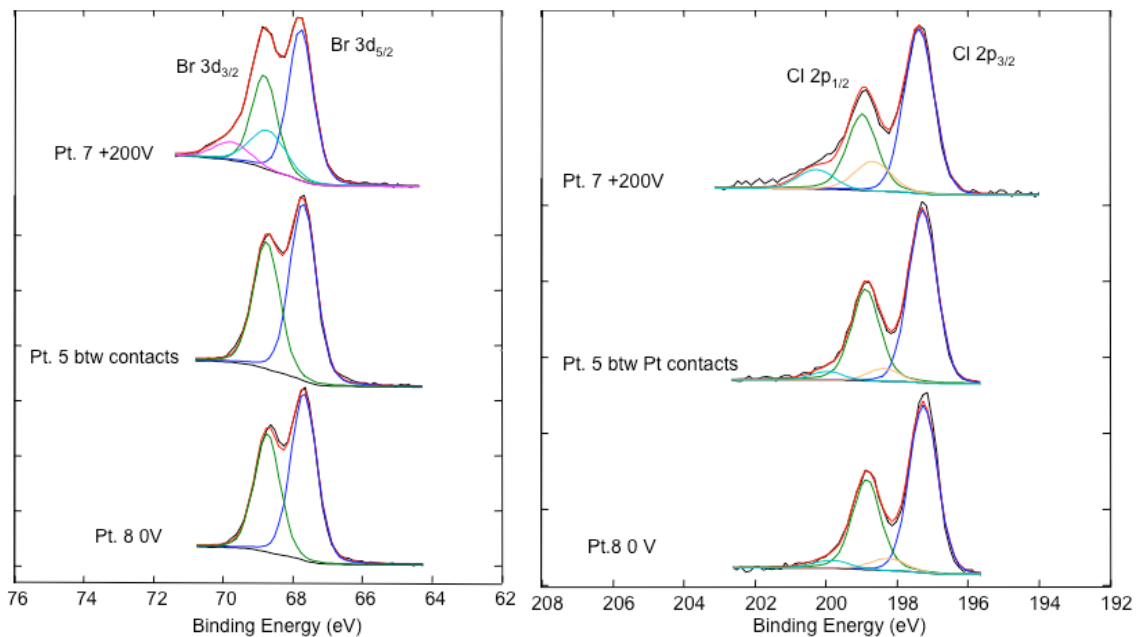


Figure 3. Br $3d_{5/2,3/2}$ and Cl $2p_{3/2,1/2}$ core-level spectra of select sites on TIBr with Pt anodes operated in air.

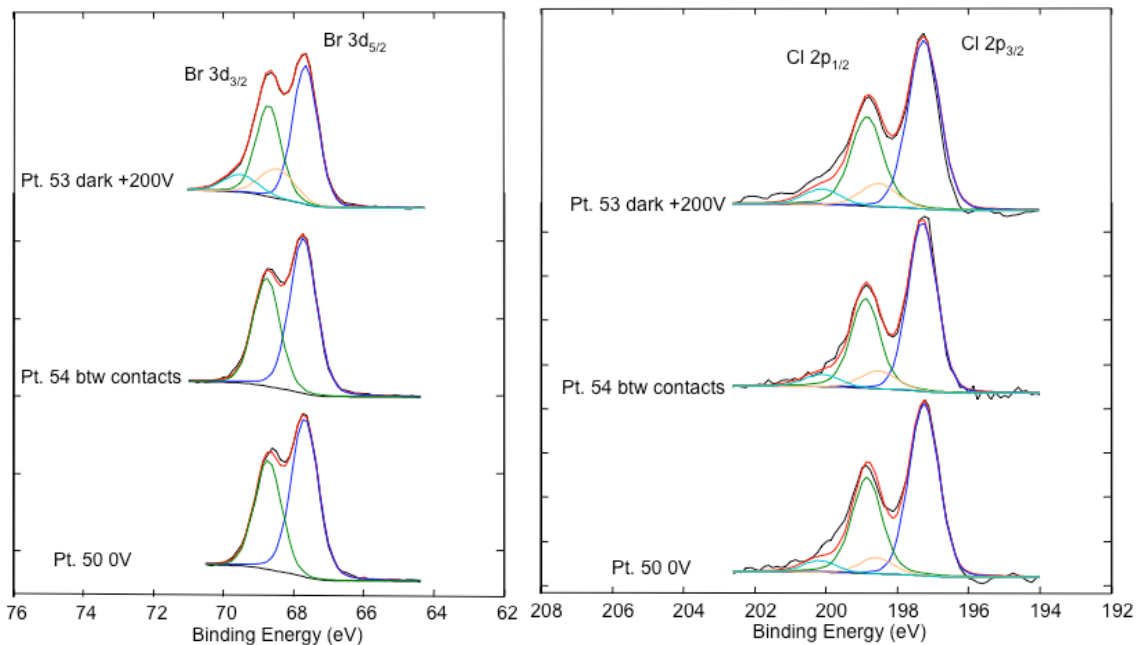


Figure 4. Br $3d_{5/2,3/2}$ and Cl $2p_{3/2,1/2}$ core-level spectra of select sites on TIBr with Pt anodes operated in N_2 .

The Br $3d_{5/2,3/2}$ and Cl $2p_{3/2,1/2}$ core-level spectra of select sites on TIBr with Pt anodes operated in air and in N_2 are shown in Figures 3 and 4. The higher binding energy components in the Br 3d spectrum for the Pt contact operated at +200V represent BrO_3^- present due to electrocatalytic activity at the interface. [11] However, the higher binding energy components in all of the Cl 2p spectra are indicative of ClO^- species, possibly due to the post etch methanol rinse in air.

The lateral surface compositional variation represented by the Cl/Br and Tl/(Br + Cl) ratios across the surfaces between the grounded Pt contact and the Pt anode operated at +200V in air and dry nitrogen are summarized in Tables 1 and 2. The Cl/Br ratio across either surface does not change predictably, but it is interesting that nearest the ground (Pt. 8 in air, Pt. 50 in N₂) they are significantly different. We also see that the Br is moving towards the positive contact as we might expect knowing that the V_{Br} is positive and moves toward the zero bias. However, we do not see a variation in the Tl/(Br + Cl) ratio at the more intermediate points presumably because they are not depleted of Br or Cl yet. However, the longer the device is operated, the larger the depleted areas should become.

Table 1. Atomic concentration ratios at marked ROI between Pt anodes operated in air.

ROI Figure 1a	Air operation	
	Cl/Br	Tl/(Br + Cl)
Background Pt. 3	1.83	1.18
Halo Pt. 8	0.87	1.35
Outside Halo Pt. 4	1.81	1.19
Between contacts Pt. 5	1.59	1.19
Between contacts Pt. 6	1.51	1.19
Between contacts Pt. 7	1.61	1.06

Table 2. Atomic concentration ratios at marked ROI between Pt anodes operated in dry nitrogen.

ROI Figure 1b	N ₂ operation	
	Cl/Br	Tl/(Br + Cl)
Halo Pt. 50	0.44	1.61
Outside Halo Pt. 51	0.68	1.24
Between contacts Pt. 53	0.61	1.16
Between contacts Pt. 54	0.56	1.24
Dark area off edge Pt. 55	0.51	1.17

Figure 5 shows the optical photomicrographs of the Mo anodes on TlBr devices operated in air and in N₂ at 200V for 7 days. The numbered regions of interest (ROI) between the contacts are shown on the photomicrographs. Again note that the spot size is 200 μm and the distance between electrodes is 3 mm.

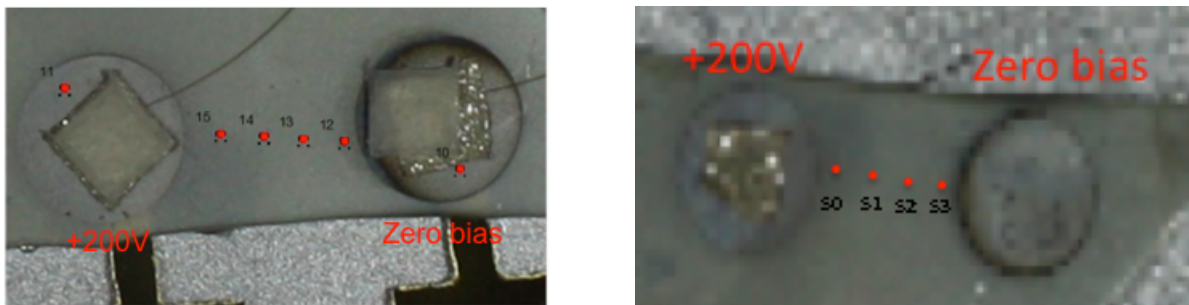


Figure 5. Photomicrographs of Mo/TlBr devices operated (a) in air and (b) in N₂.

Figure 6 presents the Tl 4f core-level spectra for Mo anodes operated in air and in N₂. Again, the curve fitting of the Tl 4f_{7/2,5/2} spin-orbit pair shows three distinct Tl species, specifically Tl⁰, Tl³⁺ as Tl₂O₃ and Tl¹⁺ in TlBr. [10] We also observe Tl on the surface of all the Mo contacts and the background is an oxidized TlBr surface.

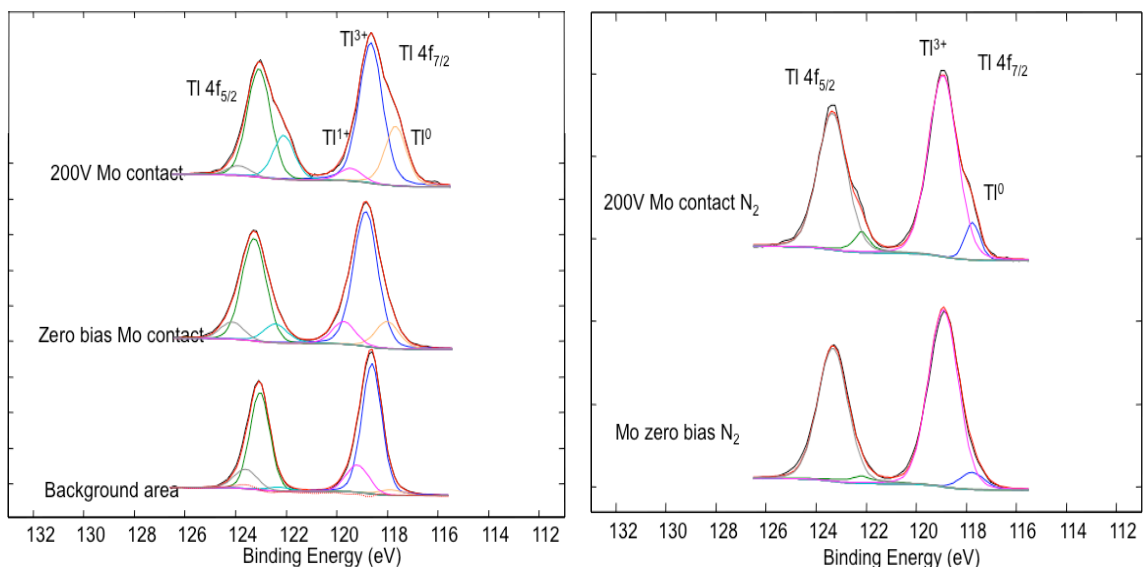


Figure 6. Ti $4f_{7/2,5/2}$ core-level spectra of select sites on TIBr with Mo anodes operated in (a) air and in (b) N_2 at 200V, ambient temperature.

Unlike Pt contacts, oxidation/reduction reactions are evident in the Mo 3d spectra as shown in Figure 7. Curve fitting of the Mo $3d_{5/2,3/2}$ spin-orbit pair for the select sites reveals three distinct oxidation states for Mo, specifically Mo^0 , Mo^{4+} in MoO_2 , and Mo^{6+} in MoO_3 . [12] Degradation of these Mo contacts in either operating environment due to electrocatalytic activity at the interface is unacceptable for reliable performance and device longevity.

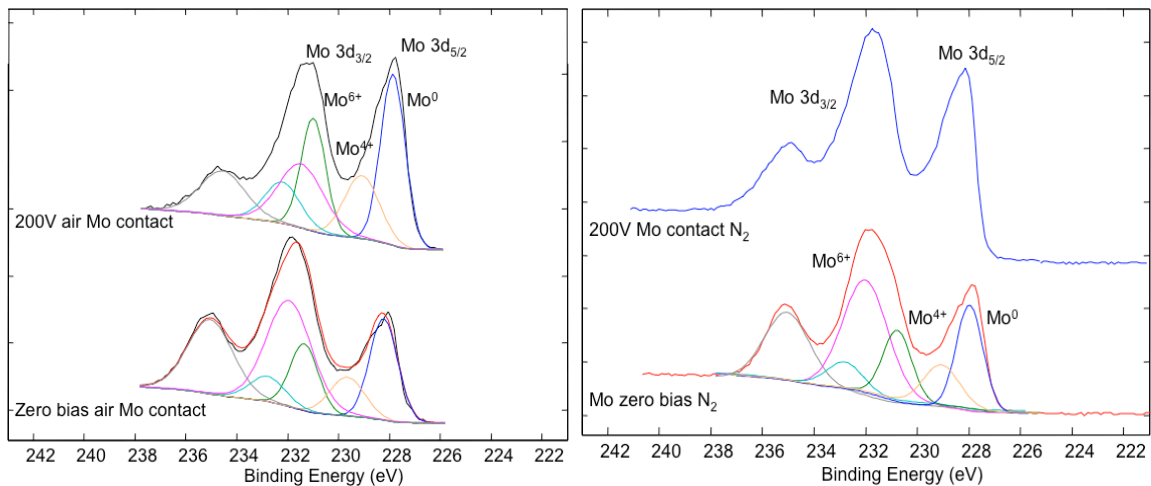


Figure 7. Mo $3d_{5/2,3/2}$ core-level spectra of select sites on TIBr with Mo anodes operated in (a) air and in (b) N_2 at 200V, ambient temperature.

Note that the Br $3d_{5/2,3/2}$ core-level spectra of select sites on TIBr with Mo anodes operated in air and in N_2 do not exhibit the higher binding energy components in the Br 3d spectrum seen for the Pt contact operated at +200V and thus are not presented here. The higher binding energy components in the Cl 2p spectra are similar to those for the Pt contacts (not presented here) and are again indicative of ClO^- species likely due to the methanol rinse in air.

The Cl/Br and Tl/(Br + Cl) ratios across the surfaces between the grounded Mo contact and the Mo anode operated at +200V in air and dry nitrogen are summarized in Tables 3 and 4. Similar conclusions can be made as before for the Pt anodes.

Table 3. Atomic concentration ratios at marked ROI between Mo anodes operated in air.

ROI Figure 1a	Air operation	
	Cl/Br	Tl/(Br + Cl)
Background Pt. 3	1.83	1.18
Halo Pt. 12	2.52	7.62
Outside Halo Pt. 13	0.96	1.21
Between contacts Pt. 14	1.14	1.19
Between contacts Pt. 15	1.04	1.21

Table 4. Atomic concentration ratios at marked ROI between Mo anodes operated in dry nitrogen.

ROI Figure 1b	N ₂ operation	
	Cl/Br	Tl/(Br + Cl)
Halo Pt. 50	0.53	1.19
Outside Halo Pt. 51	0.62	1.23
Between contacts Pt. 52	0.63	1.24
Between contacts Pt. 53	0.51	1.26

In summary, we observe that compositional changes are more prevalent near the anode and cathode of the device and we have noted that operation in N₂ reduces the oxygen content throughout.

4. CONCLUSIONS

X-ray photoelectron spectroscopy has been used to examine the surface chemistry near the metal contacts and across the surface of TlBr devices operated in air and in flowing N₂. XPS core-level spectroscopy reveals that anion substitution at the TlBr surface due to the HCl etch forms TlBr_{1-x}Cl_x with consequent formation of a shallow heterojunction. In addition, a reduction of Tl¹⁺ to Tl⁰ is observed at the metal contacts after device operation in both air and N₂ at ambient temperature. XPS results also show evidence of electrocatalytic activity at the metal contact interface. This study provides further understanding for optimizing the long-term stability and radiation response of TlBr detectors.

ACKNOWLEDGEMENTS

The work was performed under the auspices of the U.S. Department of Energy by Lawrence Livermore National Laboratory under Contract DE-AC52-07NA27344. This work has been supported by the US Department of Homeland Security, Domestic Nuclear Detection Office, under competitively awarded IAA HSHQDC-12-X-00342. This support does not constitute an express or implied endorsement on the part of the Government.

REFERENCES

- [1] Hitomi, K., Onodera, T., Shoji, T., and He, Z. "Investigation of pixelated TlBr gamma-ray spectrometers with the depth-sensing technique," Nucl. Instrum. and Meth. A **591**, 276 (2008).
- [2] Hitomi, K., Onodera, T., Shoji, T., Hiratate, Y. and He, Z. "TlBr Gamma-Ray Spectrometers Using the Depth Sensitive Single Polarity Charge Sensing Technique," IEEE Trans. Nucl. Sci. **55**, 1781 (2008).

- [3] Churilov, A.V., Ciampi, G., Kim, H., Cirignano, L.J., Higgins, W.M., Olschner, F. and Shah, K.S., "Thallium Bromide Nuclear Radiation Detector Development," *IEEE Trans. Nucl. Sci.* **56**, 1875 (2009).
- [4] Kim, H., Cirignano, L., Churilov, A.V., Ciampi, G., Higgins, W.M., Olschner, F. and Shah, K.S., "Developing Larger TlBr Detectors—Detector Performance," *IEEE Trans. Nucl. Sci.* **56**, 819 (2009).
- [5] Hitomi, K., Kikuchi, Y., Shoji, T., and Ishii, K., "Polarization Phenomena in TlBr Detectors," *IEEE Trans. Nucl. Sci.* **56**, 1859 (2009).
- [6] Oliveira, I. B., Costa, F. E., Kiyohara, P. K. and Hamada, M. M., "Influence of crystalline surface quality on TlBr radiation detector performance," *IEEE. Trans. Nucl. Sci.* **52**, 2058 (2005).
- [7] Conway, A. M., Voss, L. F., Nelson, A. J., Beck, P. R., Graff, R. T., Nikolic, R. J., Payne, S. A., Kim, H., Cirignano, L. J. and Shah, K., "Long-term room temperature stability of TlBr gamma detectors," *Proc. SPIE* 8142, 81420J (2011).
- [8] Conway, A. M., Voss, L. F., Nelson, A. J., Beck, P. R., Laurence, T., Graff, R. T., Nikolic, R. J., Payne, S. A., Kim, H., Cirignano, L. J. and Shah, K., "Fabrication of Enhanced Stability of Room Temperature TlBr Gamma Detectors," *IEEE Trans. Nucl. Sci.* **60(2)**, 1231 (2013).
- [9] Wagner, C.D., Riggs, W.M., Davis, L.E., Moulder, J.F. and Muilenberg G.E., [Handbook of X-ray Photoelectron Spectroscopy], Perkin-Elmer, Eden Prairie, (1979).
- [10] Glans, Per-Anders, Learmonth, T., Smith, K. E., Guo, J., Walsh, A., Watson, G. W., Terzi, F., Egde, R. G., "Experimental and theoretical study of the electronic structure of HgO and Tl₂O₃," *Phys. Rev.* **B71**, 235109 (2005).
- [11] Ding, L., Li, Q., Cui, H., Tang, R., Xu, H., Xie, X., and Zhai, J., "Electrocatalytic reduction of bromate ion using a polyaniline-modified electrode: An efficient and green technology for the removal of BrO₃⁻ in aqueous solutions," *Electrochimica Acta* **55(28)**, 8471-8475 (2010).
- [12] Kibsgaard, J., Chen, Z., Reneicke, B. N., and Jaramillo, T. F., "Engineering the surface structure of MoS₂ to preferentially expose active edge sites for electrocatalysis," *Nature Materials* **11**, 963 (2012).